doi:10.1246/cl.2012.934

Liquid Carbazole Substituted with a Poly(ethylene oxide) Group and Its Application for Liquid Organic Light-emitting Diodes

Korefumi Kubota,[1] Shuzo Hirata,[1] Yuki Shibano,[2] Osamu Hirata,[2] Masayuki Yahiro,[1,3] and Chihaya Adachi*[1,3]
[1]*Center for Organic Photonics and Electronics Research (OPERA), Kyushu University,*
744 Motooka, Nishi-ku, Fukuoka 819-0395
[2]*Nissan Chemical Industries, Ltd., 722-1 Tsuboi, Funabashi, Chiba 274-8507*
[3]*Institute of Systems, Information Technologies and Nanotechnologies (ISIT),*
2-1-22 Momochihama, Sawara, Fukuoka 814-0001

(Received May 11, 2012; CL-120405; E-mail: adachi@cstf.kyushu-u.ac.jp)

We report efficient carrier injection characteristics in liquid organic light-emitting diodes (OLEDs). The use of a liquid carbazole substituted with a poly(ethylene oxide) (PEO) chain provided a substantial improvement in carrier injection compared to devices constructed with carbazoles without PEO units. The external electroluminescence quantum efficiency (Φ_{EL}) of an OLED with the liquid carbazole as an emitting layer resulted in $\Phi_{EL} = 0.75\%$, 25 times higher Φ_{EL} than that of our previous liquid OLED without electrolyte.

Organic light-emitting diodes (OLEDs) using liquid molecules for the light-emitting layer, i.e., liquid OLEDs,[1] are a novel light-emitting technology presenting truly flexible and degradation-free characteristics.[2] Liquid OLEDs intrinsically prevent detachment or peeling of the liquid emitting layer from the electrodes even with hard bending and enable emission recovery by replacing a decomposed liquid emitter with a fresh liquid emitter without breaking the device structure (see Supporting Information of ref 2). However, there exists only a primitive understanding of the basic characteristics of liquid OLEDs, and fundamental performance issues such as external electroluminescence (EL) quantum efficiency (Φ_{EL}), maximum luminance, driving voltage, and device lifetime have to be largely improved. In our previous study, we reported that performance could be improved by introducing a small amount of electrolyte into the liquid emitting layer.[2] However, the introduction of electrolytes in the emitting layer always results in short device lifetimes. This behavior is similar to that seen in electrogenerated chemiluminescence (ECLs) systems with either solid-[3–5] or liquid-state[6] light-emitting layers, resulting in a serious problem for practical use.

In order to realize large device lifetimes, in this study we introduced a liquid π-conjugated molecule bearing a poly(ethylene oxide) (PEO) group as a liquid host that can improve carrier injection efficiency without electrolyte doping. Significant improvements in electron injection have been reported in polymer light-emitting diodes by introduction of PEO-containing compounds at the interface between an emitting layer and the Al cathode.[7] Herein, we have examined application of the same strategy to liquid OLED systems.

We report efficient carrier injection from electrodes into liquid carbazoles substituted with a PEO unit without using an electrolyte in liquid OLEDs. The orientation of the large dipole moment in the liquid carbazole at the interface between the liquid emitting layer and the electrode resulted in the formation of electric double layers near the electrodes, which gave rise to efficient carrier injection from the electrodes into the liquid carbazole layer. Furthermore, electron injection was greatly improved by the insertion of cesium carbonate (Cs_2CO_3) as an electron injection layer in combination with the liquid carbazole. The Φ_{EL} of the liquid OLED using the liquid carbazole with PEO substituents resulted in 0.75%, which was 25 times larger than those using the carbazole containing no PEO units.

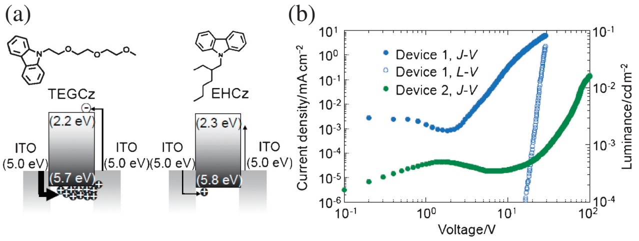

Figure 1. (a) The chemical structures of TEGCz and EHCz and energy diagrams of Devices 1 and 2. (b) *J–V–L* characteristics in Devices 1 and 2.

Figure 1a includes the chemical structures and energy level diagrams of two liquid hosts used in this study. 9-{2-[2-(2-Methoxyethoxy)ethoxy]ethyl}-9*H*-carbazole (TEGCz) was used as a liquid host, and 9-(2-ethylhexyl)carbazole (EHCz) was used as a reference. TEGCz was synthesized according to previous methods,[8] and EHCz was obtained from Sigma-Aldrich.

TEGCz and EHCz showed similar photophysical properties (see Supporting Information; SI Figures S1 and S2).[11] The maximum UV–vis absorption peaks of both neat TEGCz and EHCz liquids are located at 345 nm and have similar absorption spectra. TEGCz has two photoluminescence (PL) peaks at 371 and 410 nm, while EHCz has two major PL peaks at 387 and 407 nm. Quantum yields of PL (Φ_{PL}) in TEGCz and EHCz were 28.0% and 31.5% in the neat liquid state. The highest occupied molecular orbital (HOMO) and the lowest unoccupied molecular orbital (LUMO) levels of a neat TEGCz were 5.7 and 2.2 eV, respectively, and the HOMO and LUMO for neat EHCz were 5.8 and 2.3 eV, respectively. These results suggest that liquid OLEDs using TEGCz and EHCz should provide similar characteristics in the same device structure.

The carrier injection behavior of a liquid OLED using TEGCz as a liquid host, however, was superior to that seen with an OLED using EHCz as a liquid host. Figure 1b shows the current density (*J*)–voltage (*V*)–luminance (*L*) characteristics of two liquid OLEDs which are composed of ITO/TEGCz (720 ± 36 nm layer thickness)/ITO (Device 1) and ITO/EHCz

(649 ± 32 nm)/ITO (Device 2), respectively. The current onset in Device 1 was seen at 2.2 V, while that of Device 2 was at 10 V. The rapid increases in *J* can be ascribed to the onset of hole injection because the energy barrier between the work function of an ITO anode (5.0 eV) and the HOMO levels of TEGCz (5.7 eV) and EHCz (5.8 eV) is smaller than that between the work function of an ITO cathode (5.0 eV) and the LUMO levels of TEGCz and EHCz (2.2–2.3 eV). Also, the lack of electroluminescence suggests single carrier injection in their *J*–*V* characteristics. Thus, we conclude that hole injection at the interface of ITO/TEGCz is significantly improved over that at the interface of ITO/EHCz, even though there is no difference in the estimated energy barrier, as shown in Figure 1a. The differences of the carrier injection barrier between TEGCz and EHCz cannot be explained by the energy diagrams since the HOMO and LUMO levels of TEGCz and EHCz are almost the same. Furthermore, blue emission with $EL_{max} = 440$ nm emerged over 15 V as shown in Figure 1a in Device 1 while no emission was observed in Device 2, even with the maximum voltage of 100 V, indicating that electron injection into a TEGCz layer is also superior to that into a EHCz layer. Furthermore, we note that a nearly identical improvement of carrier injection was observed when each of the liquid carbazoles having different PEO chain lengths (1–4 ethylene oxide units) was used as the liquid host (see SI Figure S3[11]).

To investigate the mechanism of the improvement of carrier injection with a TEGCz layer compared to the EHCz layer, the frequency dependence of capacitance in TEGCz and EHCz layers between two ITO electrodes was evaluated. Figure 2 shows that the capacitance of TEGCz increased in the low frequency region (i), while the capacitance of EHCz was almost constant (ii). Such behavior is suggestive that TEGCz contains ionic impurities. While we tried to produce the highest possible purity TEGCz, analysis by ion chromatography indicated that TEGCz contained a trace amount of Cl^- ions in addition to a large amount of H_2O as shown in the inset of Figure 2. Although the origin of Cl^- ions can be attributed to sodium chloride used in the synthetic process of TEGCz, they could not be removed after several column chromatography treatments. Karl Fischer analysis also revealed that a large amount of H_2O (1000–2000 ppm) is dissolved into TEGCz in air, while EHCz contains virtually no H_2O in air (the inset table of Figure 2). The H_2O could not be removed with conventional purification procedures. The unremovable H_2O in TEGCz is due to the strong hydrophilicity of the PEO unit that leads to H_2O contamination during the synthetic procedure. Thus, PEO-substituted liquid carbazoles always show a capacitance increase at low frequency regions because of the presence of H_2O. The magnitude of the low-frequency capacitance increased with increasing PEO chain length (see SI Figure S5[11]). This suggests that the amount of H_2O is proportional to the number of PEO monomers.

The frequency dependence in the high-frequency range indicates that TEGCz has a larger dielectric constant than EHCz. The capacitance of a liquid material does not display a frequency dependence at frequencies above 10^4 Hz even if ionic components are contained within the liquid layer, since the rapid switching of the alternating current (AC) bias is too fast for ions to reach each electrode. Therefore, the capacitance value in the high-frequency range provides information on the intrinsic dielectric constant of the liquid.

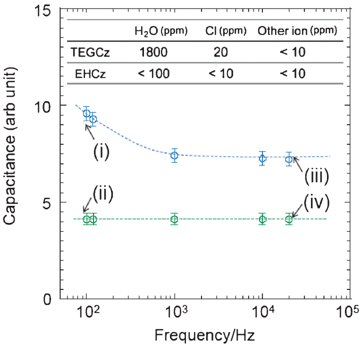

	H_2O (ppm)	Cl (ppm)	Other ion (ppm)
TEGCz	1800	20	< 10
EHCz	< 100	< 10	< 10

Figure 2. Frequency dependence of capacitance in ITO/TEGCz (10 ± 0.5 μm)/ITO (blue symbols) and ITO/EHCz (10 ± 0.5 μm)/ITO (green symbols).

Figure 2a shows that the capacitance of TEGCz (iii) is 1.76 ± 0.18 times larger than that of EHCz in the high frequency region (iv), indicating that TEGCz has a larger dipole moment than EHCz. This is reasonable because the average of dipole moment of various conformations estimated by CONFLEX formation analyses and DFT (Gaussian 09, Revision A.02[9] (B3LYP/6-31G*)) calculations in TEGCz ($\langle\mu\rangle = 2.32$ D) is larger than that in EHCz ($\langle\mu\rangle = 1.91$ D) (see SI Figures S6 and S7[11]). It has been reported that PEO presents a large dipole moment because of the unshared electron pairs of oxygen atom of the PEO chain.[10]

Based on the frequency-dependent capacitance results and the analysis of impurities, there are two probable mechanisms which may affect the efficient carrier injection of TEGCz. In the first model, the small ionic impurities (such as Cl^-, H^+, and OH^-) are driven toward each electrode and form an electric double layer at the interface between TEGCz layer and the electrodes when direct current (DC) bias is applied between the two ITO electrodes. This results in carrier injection enhancement because of a tunneling effect (Figure 3a(i)).[4] In the second model, under a DC bias the orientation of the large TEGCz dipole moment induces the formation of electric double layers at the interface between the TEGCz layer and each electrode, resulting in the same enhancement of carrier injection (Figure 3a(ii)).

Here, we confirmed that the improvement of carrier injection in TEGCz can be ascribed to the latter model. ITO/TEGCz (1590 ± 80 nm)/ITO (Device 3), ITO/EHCz (1420 ± 71 nm)/ITO (Device 4), ITO/EHCz doped with 1780 ppm H_2O (1380 ± 69 nm)/ITO (Device 5), and ITO/EHCz doped with 20 ppm tetrabutylammonium chloride as a source of Cl^- ions (1360 ± 68 nm)/ITO (Device 6), were fabricated and confirmed the contribution to carrier injection by inclusion of small amounts of Cl^- ions and H_2O. Figure 3b shows *J*–*V*–*L* and Φ_{EL}–*J* characteristics of Devices 3 to 6. Since the difference between Devices 4 and 5 is only the existence of H_2O, comparison of the carrier injection behavior of these devices shows the effect of doping a small amount of H_2O into a nonionic liquid. Similarly, comparison of Devices 4 and 6 shows the effect of doping Cl^- ions into the liquid layer. In the pure EHCz case (Device 4), while hole injection occurs at voltages higher than 20–30 V (Figure 3b(A)), no electron injection was observed. Devices 5 and 6 showed the onset of hole injection at 30 and 10 V ((B) and (C)) and that of electron injection at 70 and 30 V ((D) and (E)). These observations indicate that ionic doping

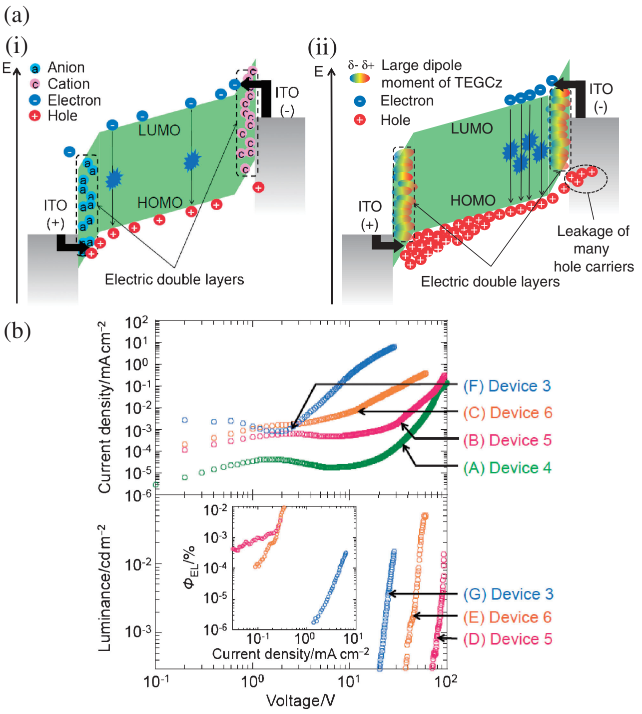

Figure 3. (a) Two possible carrier injection models in Device 1. (i) Formation of a dielectric double layer by ionic impurities contained in TEGCz. (ii) Formation of a dielectric double layer due to the orientation of the large TEGCz dipole moment. (b) J–V–L (upper) and Φ_{EL}–J (lower) characteristics in Devices 3 to 6 when ionic species were doped into a nonionic liquid semiconducting layer. Blue, green, red, and orange symbols represent Devices 3, 4, 5, and 6, respectively.

improves carrier injection, which is consistent with previous reports.[3–5] In contrast, the onset of hole injection was seen at 2.4 eV in Device 3 using TEGCz ((F)) and was drastically different from that in Devices 5 and 6. Furthermore, Φ_{EL} in Device 3 was appreciably lower than in Devices 5 and 6 (Inset in Figure 3b). These results indicate that the presence of the PEO chain strongly enhanced hole injection and successive hole leakage to the cathode side in Device 3, leading to lower Φ_{EL} (Figure 3a(ii)). On the other hand, small amounts of ionic impurities have only a limited effect for both hole and electron injections (Figure 3a(i)). Therefore, the significant improvement of carrier injection into TEGCz suggests the formation of the electric double layers due to the orientation of the large TEGCz dipole.

In Device 1, Φ_{EL} was limited to 10^{-3}% because of poor electron injection from the ITO cathode to the TEGCz layer (blue symbols in the inset of Figure 3b). High Φ_{EL} may be achieved by inserting an electron injection layer such as $\mathrm{Cs_2CO_3}$ which redox potential is 3.1 eV between the TEGCz layer and the ITO cathode. ITO/poly(3,4-ethylenedioxythiophene)poly(styrenesulfonate) (PEDOT:PSS) (30 nm)/1 wt %-5,6,11,12-tetraphenyltetracene (rubrene), 99 wt %-TEGCz (680 ± 34 nm)/$\mathrm{Cs_2CO_3}$ (5 nm)/ITO (Device 7) was fabricated using $\mathrm{Cs_2CO_3}$ as an electron injection layer. In Device 7, rubrene was used to increase Φ_{PL}.

The blue symbols of Figure 4 show J–V–L and Φ_{EL}–J characteristics of Device 7. Although the onsets of hole and electron injections occurred at 2–3 and 16 V, respectively, in Device 1 (Figure 1a, blue plots), both hole and electron injections occurred at 2.8 V in Device 7 (Figure 4a, blue plots). As a reference for Device 7, ITO/PEDOT:PSS (30 nm)/1 wt %-rubrene, 99 wt %-EHCz (649 ± 32 nm)/$\mathrm{Cs_2CO_3}$ (5 nm)/ITO (Device 8) was fabricated. The onset of EL in Device 7 (2–3 V) occurred at a lower voltage value than in Device 8 (7 V) (Figure 4a). Thus, in Device 7, the applied voltage effectively affected to pull electrons in the TEGCz layer. Consequently, the effective hole and electron injections in Device 7 result in a Φ_{EL} value of 0.75%, which is 25 times larger than that in Device 8 ($\Phi_{\mathrm{EL}} = 0.03\%$) (Figure 4b). We note that $\Phi_{\mathrm{EL}} = 0.75\%$ is a vast improvement over previously reported liquid OLEDs containing electrolyte ($\Phi_{\mathrm{EL}} = 0.31\%$)[2] and liquid ECLs ($\Phi_{\mathrm{EL}} = 0.20\%$).[6]

In summary, efficient carrier injection into a liquid emitting layer was demonstrated without the addition of an electrolyte. PEO-substituted carbazole was used as a liquid emitting layer and displayed efficient carrier injection properties without electrolyte doping. The efficient carrier injection was ascribed to the formation of electric double layers at the electrode interfaces which are induced by the orientation of the large dipole of PEO units in TEGCz. Furthermore, by using TEGCz and $\mathrm{Cs_2CO_3}$ as electron injection layers improved the carrier recombination balance, resulting in a Φ_{EL} of 0.75%.

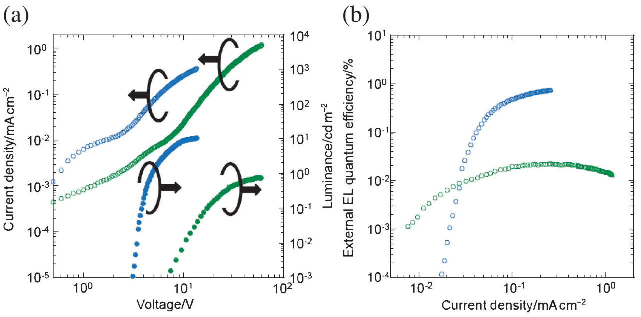

Figure 4. Enhancement of EL characteristics using $\mathrm{Cs_2CO_3}$ as an electron injection layer. J–V–L (a) and Φ_{EL}–J (b) characteristics in Devices 7 and 8. Blue and green symbols show data for Devices 7 and 8, respectively.

References and Notes

1 D. Xu, C. Adachi, *Appl. Phys. Lett.* **2009**, *95*, 053304.
2 S. Hirata, K. Kubota, H. H. Jung, O. Hirata, K. Goushi, M. Yahiro, C. Adachi, *Adv. Mater.* **2011**, *23*, 889.
3 Q. Pei, G. Yu, C. Zhang, Y. Yang, A. J. Heeger, *Science* **1995**, *269*, 1086.
4 J. C. deMello, *Nat. Mater.* **2007**, *6*, 796.
5 H. J. Bolink, E. Coronado, R. D. Costa, E. Ortí, M. Sessolo, S. Graber, K. Doyle, M. Neuburger, C. E. Housecroft, E. C. Constable, *Adv. Mater.* **2008**, *20*, 3910.
6 N. Itoh, *Materials* **2010**, *3*, 3729.
7 T.-H. Lee, J.-C.-A. Huang, G. L. Pakhomov, T.-F. Guo, T.-C. Wen, Y.-S. Huang, C.-C. Tsou, C.-T. Chung, Y.-C. Lin, Y.-J. Hsu, *Adv. Funct. Mater.* **2008**, *18*, 3036.
8 F. Tran-Van, T. Henri, C. Chevrot, *Electrochim. Acta* **2002**, *47*, 2927.
9 M. J. Frisch et al., *Gaussian 09, Revision A.02*, Gaussian, Inc., Wallingford CT, **2009**.
10 N. Yamaguchi, M. Sato, *Polym. J.* **2009**, *41*, 588.
11 Supporting Information is available electronically on the CSJ-Journal Web site, http://www.csj.jp/journals/chem-lett/index.html.